A Design of Compact Multi-harmonic Suppression LTCC Bandpass Filter

by Xu-Guang Wang

Under the Supervision of Prof. In-Ho Kang

Department of Radio Science and Engineering

in the Graduate School

of

Korea Maritime University

July 2008

A Design of Compact Multi-harmonic Suppression LTCC Bandpass Filter

by Xu-Guang Wang

Here is approved that this is the thesis submitted in partial satisfaction of the requirements for degree of

MASTER

in Radio Science and Engineering in the Graduate School of

Korea Maritime University

Approved by: Prof. Ki-Man Kim

Prof. Young Yun

Prof. In-Ho Kang

Committee in Charge

Contents

Nomenclature

f :	Frequency
f_0 :	Center frequency
Y_0 :	Characteristic admittance
Z_0 :	Characteristic impedance
Z_{0e} :	Even-mode characteristic impedance
Z_{0o} :	Odd-mode characteristic impedance
J_{ij} :	Admittance inverter parameter
C :	Capacitance
L :	Inductance
w :	Fractional bandwidth
g_j :	Prototype filter element value
l_j :	Susceptance slope parameter
θ :	Electrical length
λ :	Wavelength
ω :	Angular frequency
K :	Coupling coefficient
S_{11} :	Return loss
S_{21} :	Insertion loss

List of Tables

List of Figures

Abstract

Filters are key components in RF front-end circuits and usually occupy much of the volume of the systems. Thus, reducing the size of filters is the main challenge in making RF systems compact. In addition to compact size, high performance is also desired. The presence of harmonics or spurious passbands is a fundamental limitation of microwave circuits, which can seriously degrade their performance and can be critical in certain applications.

In this thesis, a simple and effective filter design method is proposed based on the structure of parallel short-ended coupled-line with capacitive loading for size reduction and ultra-broad rejection of the spurious passbands. It is achieved by adding lumped capacitors to the conventional coupled-line section such that the required length of the coupled-line can be largely reduced while maintaining approximately the same characteristics around the center frequency, and meanwhile the spurious passbands are excellently suppressed. In addition, the introduction of a cross-coupling capacitor into the miniaturized couple-line can create a transmission zero at the 2nd harmonic frequency for enhanced frequency selectivity and attenuation level. The aperture compensation technique is also applied to achieve a strong coupling in the coupled-line section.

In order to examine the feasibility of the proposed structure, such a

compact two-stage bandpass filter operating at 2.3 GHz with a fractional bandwidth of 10% was designed and realized with LTCC technology. Measured results are also provided, from which attractive features are observed experimentally as to size reduction and multi-harmonic suppression.

요 약

대역 통과 필터는 RF 송수신 단의 중요한 소자이며 일반적으로 시스템에서 많은 면적을 차지한다. 따라서 필터의 크기를 줄이는 것은 무선 송수신 시스템의 크기를 줄이는데 매우 중요한 부분이라 할 수 있다. 또한 시스템의 비선형성으로 인하여 발생하는 불요파는 무선 통신 회로의 성능을 악화시키는 것으로써 통신 시스템의 기본적인 제약으로 작용한다. 따라서 대역 통과 필터는 이러한 불요파를 차단하는 중요한 역할을 하게 된다.

본 논문에서는 단순하고 효율적인 필터설계 기술을 제공한다. 이러한 기술은 소형화 및 불요파 억제를 위하여 끝이 콘덴서로 연결되어 있고 나머지 한쪽 끝이 단락 되어 있는 소형화된 결합선로의 구조를 가진다. 또한 소형화된 결합선로 중간에 콘덴서를 연결함으로써 두 번째 하모닉을 차단하고 선택도를 높이는 효과를 실현하였다. 접지 평면 중간에 접지부분을 없애는 기법을 이용하여 결합선로의 결합도를 높이는 것을 실현하였다.

제안된 구조를 실현하기 위하여 2.3 GHz, 대역폭 10% 에 동작하도록 초소형 2 단 대역통과 필터를 LTCC 제조 기법을 이용하여 설계하고 제작하였다. 측정된 결과는 예측치와 거의 일치하였으며 필터의 소형화, 하모닉 성분 억제 등을 구현하였다.

CHAPTER 1 Introduction

Filters play important roles in many RF/microwave applications. They are widely used to control the frequency response at a certain point in a microwave system by providing transmission at frequencies within the passband of the filter, and attenuation in the stopband of the filter, because the electromagnetic spectrum is limited and has to be shared. In recent years, the microwave filters with ever more stringent requirements—smaller size, higher performance, lighter weight, and lower cost have widely attracted attentions of the microwave and millimeter-wave engineers.

Being one of the essential building blocks for communication systems, bandpass filters can pass the desired frequencies, reject the unwanted signals, and suppress the harmonics or spurious responses as well. The rapid growth of wireless communication systems has led to a great increasing demand for compact microwave filters since most mobile platforms have a limited space for the required filters. The focus of this thesis is placed on the design issues of the bandpass filter with compact size and high performance.

1.1 Background and motivation

The realization of compact microwave bandpass filters with high

performance has been the focus of great deal of research and industrial pursuit for over two decades. Since the parallel coupled-line microstrip filter was proposed by Cohn in 1958 [1], it has been widely used in microwave applications due to its planar structure, simple synthesis procedures and fabrication facility. Nevertheless, these conventional parallel coupled-line filters are too large to apply to mobile communication systems. So far, various approaches have been presented for the filter miniaturization. For instance, folded hairpin resonator filters [2]-[4] and stepped-impedance filters [5]-[7] were investigated and developed to reduce the size, and slow wave open-loop resonator filters have also been considered as an effective solution to the problem of filter size [8]-[10]. Using the above proposed methods, relatively compact bandpass filter can be achieved. However, they just miniaturize the overall filter size to a certain extent and still take up a large circuit space, especially at lower frequency.

Another critical disadvantage of the traditional parallel coupled-line filters is the existence of a spurious passband at twice of the center frequency ($2\ f_0$), which may seriously degrade the attenuation level in the upper stopband and the passband response symmetry. This undesired passband is associated to the nonhomogeneous nature of the dielectric surrounding the conductors which leads to unequal phase velocity of the even-mode and odd-mode (even-mode velocity is slower). The unequal modal phase velocities at $2\ f_0$ cause the first spurious passband. To tackle this problem, many studies have been reported in the literature. The parallel-coupled microstrip filter with over-coupled end stages was proposed to extend the electrical length of odd-mode [11]. In wiggly-line

filter structure, wave impedance using the continuous perturbation of the width of the coupled-line can be modulated so that the spurious passband is rejected [12]. Meandered parallel coupled-line filters also effectively suppress the spurious passband [13]. A proper height of substrate suspension can be used to equalize the even- and odd-mode phase velocities in the parallel coupled-line filters [14]. However, the first spurious passband of these published filters is just moved to the higher frequency, not eliminated, and the upper spurious passbands still exist in these filters. Furthermore, the above mentioned techniques rely on complex design/optimization procedures. More recently, the photonic bandgap (PBG) structure and defected ground structure (DGS) have been introduced as a popular mean to achieve harmonic suppression [15], [16]. However, owing to the periodic structure of the PBG or DGS, this type of filter suffers from its large circuit area and specific circuit configurations, which seriously hinders the application to wireless communication systems.

On the other hand, filters have been a hot topic for any emerging new materials and fabrication techniques and they are still a very active topic today. The main reason is that filter performance highly depends on the unloaded quality factor of the resonators, which is closely related to material quality and fabrication techniques. With new materials and fabrication techniques, people can not only improve the filter performance but also reduce filter size and make it more integrated. In recent years, the Low Temperature Co-fired Ceramic (LTCC) technology has proven its extreme efficiency for compact and reliable radio-frequency (RF) modules for wireless communications. It can offer many advantages in

achieving higher packaging densities for RF/microwave integrated circuits such as high-precision three-dimensional (3-D) structuring and vertical integration of the circuits, making the miniaturized and low-cost design possible. Moreover, on account of the high unloaded quality factor of LTCC material, it is a very good option for realizing highly integrated modules and microwave filters those present the satisfactory electrical performance [17]-[19].

In this thesis, a novel bandpass filter design approach for size miniaturization and multi-harmonic suppression is demonstrated using capacitive loading of parallel short-ended coupled-line structure. The method of adding lumped capacitors to the conventional coupled-line section can largely reduce the required length of coupled-line while maintaining approximately the same characteristics around the center frequency and effectively suppress the spurious passbands. In addition, by introducing the cross-coupling capacitor between the input and output ports into the miniaturized coupled-line section, a transmission zero can be generated to achieve better frequency selectivity and wide multi-harmonic suppression. This method is general and geometry-independent, thus can be applied to any type of bandpass filter design. Specifically, such a compact two-stage bandpass filter working at 2.3 GHz with a transmission zero at 2nd harmonic frequency has been implemented in a multilayer LTCC substrate for experimental demonstration. Beyond the advantage of excellent multi-harmonic suppression better than -40 dB up to 4 f_0, where f_0 is the center frequency, the fabricated bandpass filter has a small size of 10 × 7 × 2.2 mm^3 and low insertion loss of -1.2 dB. The measured results agree well

with the simulation, which demonstrates that the proposed filter has great application potential.

1.2 Organization of the thesis

The thesis is organized as follows. Chapter 1 has briefly described the background, purpose, and direction of this work. Chapter 2 reviews the traditional bandpass filter design theory and builds up the novel filter synthesis method for size reduction and multi-harmonic suppression. Chapter 3 presents the complete design procedure of such a two-stage compact LTCC bandpass filter, including simulation in ADS and HFSS, optimization, and measurement. Finally, chapter 4 gives the conclusion of this work.

CHAPTER 2 Filter Design Theory

Filter design is one of the oldest topics in microwave engineering. Filter synthesis can be started from a lumped element low-pass prototype circuit which consists of shunt (series) capacitors and series (shunt) inductors. This low-pass prototype serves as a basis for any low-pass, high-pass, bandpass and bandstop filters. The well-known maximally flat filter and Chebyshev filter prototype values are tabulated in [20]. Low-pass prototypes can be transformed to high-pass, bandpass and bandstop filters using transformations described in [20]. In this thesis, we will focus on bandpass filter design and the size reduction issues based on capacitive loading of parallel short-ended coupled-line as well as multi-harmonic suppression.

2.1 Traditional bandpass filter design

Bandpass filters may be obtained through a ladder combination of series and shunt resonators. In microwave filter realization, however, it is sometimes difficult to design both series and shunt type of resonators. Therefore, they may be obtained by combining only one type of resonators through impedance inverters or admittance inverters that would be more convenient and practical for implementation with microwave structures. This kind of filter synthesis approach using network theory has been well developed in [20]. As an example, Fig. 2.1 shows the

generalized bandpass filter circuit using admittance inverters.

An ideal admittance inverter is a two-port network that exhibits such a property at all frequency that if an admittance Y_2 is connected at one port, the admittance Y_1 seen looking in the other port is

$$Y_1 = \frac{J^2}{Y_2} \tag{2.1}$$

One of the simplest forms of the inverter is a quarter-wavelength transmission line with characteristic admittance of Y_0. Observe that such a line obeys the basic admittance inverters definition in (2.1) and that it will have an inverter parameter of $J = Y_0$.

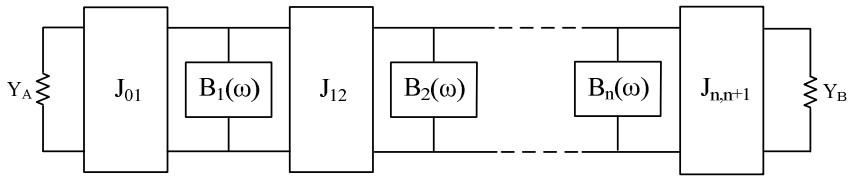

Fig. 2.1 Equivalent circuit model of the generalized bandpass filter using admittance inverters.

The J inverter values of this generalized bandpass filter are given by [20]

$$J_{01} = \sqrt{\frac{Y_A l_1 w}{g_0 g_1 w_1'}} \tag{2.2}$$

$$J_{j,j+1}\,|_{j=1\ to\ n-1} = \frac{w}{w_1'}\sqrt{\frac{l_j l_{j+1}}{g_j\, g_{j+1}}} \tag{2.3}$$

$$J_{n,n+1} = \sqrt{\frac{Y_B\, l_n\, w}{g_n g_{n+1} w_1'}} \tag{2.4}$$

where $w_1' = 1$, w is the fractional bandwidth, Y_A and Y_B are source and load conductance, respectively, g_j is the prototype filter element value and l_j is the susceptance slope parameter given by

$$l_j = \frac{\omega_0}{2}\frac{dB_j(\omega)}{d\omega}\,|\,\omega = \omega_0 \qquad (j = 1, 2, \ldots., n) \tag{2.5}$$

For a simple shunt LC resonator, equation (2.5) is reduced to $l_j = \omega_0 C_j = \frac{1}{\omega_0 L_j}$.

2.2 Size reduction method

In conventional filter prototypes, the values of J_{ij} are the functions of the resonator parameters and not arbitrary and equal. However, to simplify the miniaturized filter circuit, we will adopt identical inverters instead of different inverters, making the physical realization much easier. This simplification will not degrade the filter performance which can be proven in the following design procedures. Shown in Fig. 2.2 (a) is a possible second-order generalized bandpass filter topology with all three

inverter values being 0.02. Since the impedance of input and output matching quarter-wavelength transmission line is equal to the system impedance, these two transmission lines can be neglected and the second-order bandpass filter can be connected directly to the input and output ports. Consequently, the filter model to be miniaturized is obtained, illustrated in Fig. 2.2 (b).

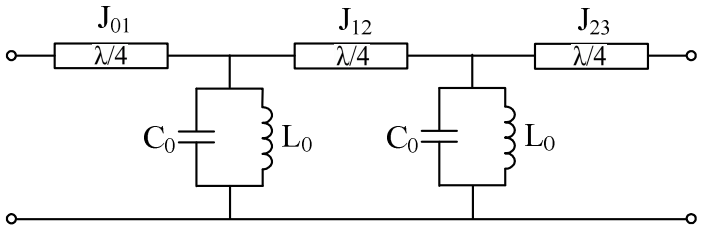

(a)

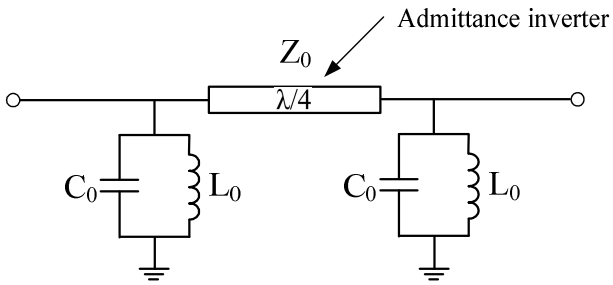

(b)

Fig. 2.2 Circuit model of a second-order generalized bandpass filter using admittance inverters (a) and its simplified version under the assumption of identical admittance inverter values being 0.02 (b).

And then the size reduction method will be briefly introduced here. As is well known, the λ/4 transmission line can be made equivalent to a lumped circuit, as given in Fig. 2.3, and the value of C_1 is given by

$$C_1 = \frac{1}{\omega Z_0} \tag{2.6}$$

where Z_0 is the characteristic impedance of the quarter-wavelength transmission line and ω is the angular frequency.

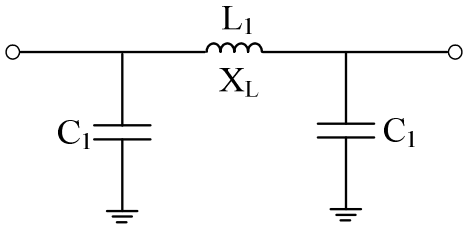

Fig. 2.3 The equivalent lumped circuit of the quarter-wavelength transmission line.

Replacing the admittance inverter with the equivalent lumped circuit, the generalized bandpass filter can be expressed as Fig. 2.4. Next step, the dotted network can further be made equivalent to the parallel short-ended coupled-line section with electrical length of θ in Fig. 2.5 (a) and (b) when (2.7) and (2.8) are satisfied [21].

$$X_0 = Z_{0e} \tan\theta \tag{2.7}$$

$$X_L = \frac{2Z_{0e}Z_{0o}}{Z_{0e} - Z_{0o}} \tan\theta \tag{2.8}$$

where Z_{0e}, Z_{0o} are even- and odd-mode impedances of the parallel coupled-line, respectively.

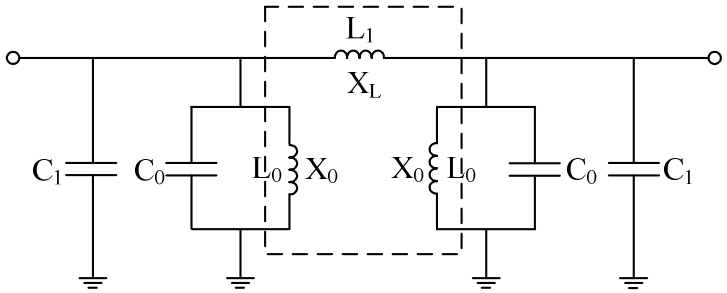

Fig. 2.4 The equivalent lumped circuit of the original generalized bandpass filter.

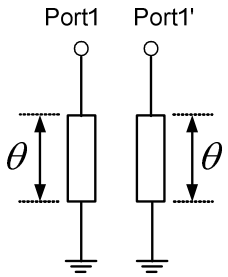

(a)

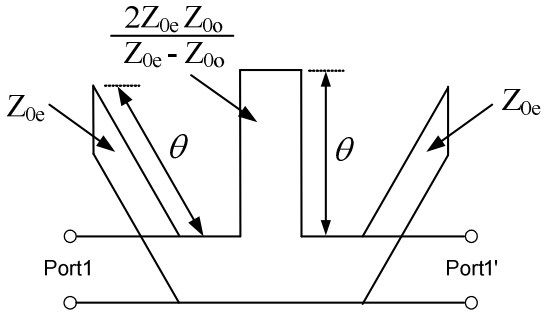

(b)

Fig. 2.5 The parallel short-ended coupled-line (a) and its equivalent network (b).

Fig. 2.6 shows the initial miniaturized bandpass filter configuration based on the transformation described above and the value of C_0 can be deduced from (2.7) as:

$$C_0 = \frac{1}{\omega Z_{0e} \tan\theta} \tag{2.9}$$

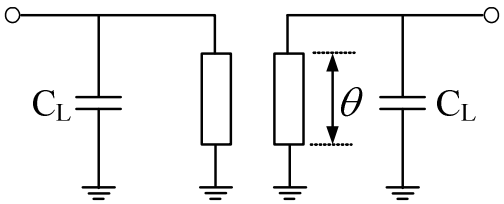

$$C_L = C_0 + C_1$$

Fig. 2.6 The initial miniaturized one-stage bandpass filter configuration.

In the following simulation and fabrication, one capacitor C_L will be used as the sum of C_0 and C_1, and if defining $Z' = \frac{2Z_{0e}Z_{0o}}{Z_{0e} - Z_{0o}}$ as the characteristic impedance of the coupled-line, then with (2.8) we get:

$$Z' = \frac{Z_0}{tan\,\theta} = \frac{2Z_{0e}Z_{0o}}{Z_{0e} - Z_{0o}} \tag{2.10}$$

When the electrical length θ is very small for compact size, Z' becomes very large, for instance, Z' is 407 Ω when θ = 7º and Z_0 = 50 Ω. This large Z' can be easily achieved by making Z_{0e} and Z_{0o} nearly the same.

2.3 Realization of transmission zero

The attenuation level at the 2nd harmonic frequency can further be improved by employing the cross-coupling capacitor C_C in the miniaturized coupled-line section, as shown in Fig. 2.7 (a), which can create a transmission zero, such that a sharper falloff rate at right passband edge is obtained. The presence of this transmission zero (as long as it is not too close to the passband) does not change the passband characteristics of the filter too much. Fig. 2.7 (b) depicts the equivalent lumped circuit of the final miniaturized one-stage bandpass filter, from which we can see that it is the dotted resonator that provides a transmission zero in the upper stopband. Therefore, the location of this transmission zero may easily be adjusted by varying the capacitor value. By selecting the capacitor value properly, it can be designed to achieve a transmission zero for suppressing the 2nd harmonic with same passband

response as the proposed filter in last section. Furthermore, this transmission zero can also suppress the spurious response resulted from cascading, as detailed explained in the next chapter. Tang [18] adopted a similar circuit structure to design LTCC bandpass filter, diplexer, and triplexer with transmission zero and he analyzed the proposed structure using the technique of the immittance inverter. The exact value of C_C was derived in his literature as

$$C_C = \begin{cases} \dfrac{J_{12}}{\omega_0 - \omega_{z1}\dfrac{\tan\theta_{z1}}{\tan\theta_0}} & \textit{when the transmission zero is in lower stopband} \\ \dfrac{J_{12}}{\omega_{z1}\dfrac{\tan\theta_{z1}}{\tan\theta_0} - \omega_0} & \textit{when the transmission zero is in upper stopband} \end{cases} \tag{2.11}$$

where θ_0 and ω_0 are electrical length and angular frequency at the center frequency, respectively; θ_{z1} and ω_{z1} are electrical length and angular frequency at the transmission zero frequency, respectively.

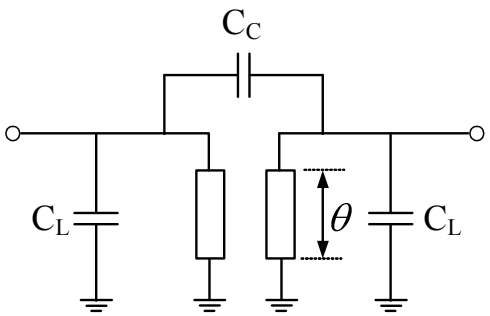

(a)

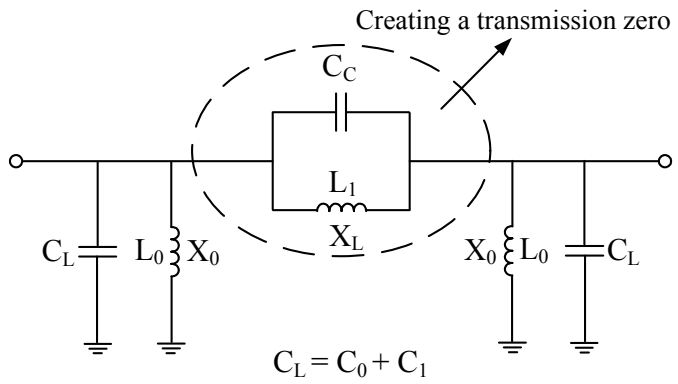

(b)

Fig. 2.7 The final structure of the miniaturized one-stage bandpass filter with a transmission zero (a) and its equivalent lumped circuit (b).

Here, we also adopted this formula for the calculation of C_C to avoid the time-consuming iterative procedure and facilitate the filter design. According to the equation, the transmission zero can be arbitrarily distributed in the lower and upper stopband. The proposed accurate and explicit equation provides the element value estimation to achieve the required filter specifications. Then, these values are substituted into a full-wave EM simulator for fine-tuning to include the LTCC substrate conductor losses and cross-layer coupling.

Note that the insertion of this cross-coupling capacitor will change the coupling situation of the coupled-line. Now it is coupled not only electromagnetically but also electrically through C_C, while the original coupled-line is coupled only electromagnetically. Consequently, some

modification of the parameters of coupled-line is necessary. This is not a troublesome problem since we can get the help of Agilent Advanced Design System (ADS) to find the proper new parameters quickly, which will also be detailed expounded in the next chapter. Usually, in this case, the slot between two striplines is small in comparison with that for a conventional parallel coupled-line, which means that the electromagnetic coupling is larger.

2.4 Aperture compensation technique

To realize the tightly coupled line section, a usual technique is to reduce the width or slot of the coupled-line in question. Unfortunately, it may lead to a serious degradation of filtering behavior, for example, low Q-factor and high insertion loss. And also, it may cause some difficulties in design and fabrication due to the limitation of the minimum slot between the coupled stripline conductors in realization process.

As an alternative approach, the aperture compensation technique is applied in this thesis. Fig. 2.8 depicts a schematic layout of the coupled striplines, in which a wide aperture with rectangular configuration is formed on both the ground planes over and underneath the coupled striplines in the center. This aperture has an effect on the equivalent capacitances between the strip conductors and the ground, as shown in Fig. 2.8. With this aperture, the even-mode characteristic Z_{0e} of the coupled striplines becomes larger as the effective distance between the strip conductors and the ground gets longer [22], which can be seen in Fig. 2.8. However, the odd-mode characteristic Z_{0o} remains nearly the same as its value is mainly determined by C_{12} that is scarcely influenced by

the aperture. As a result, the coupling coefficient K could be increased tremendously, which relieves the fabrication limitation and realizes enhanced coupling in the miniaturized coupled-line section.

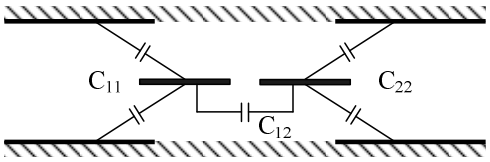

Fig. 2.8 The equivalent capacitance network of the coupled striplines.

CHAPTER 3 Simulation, Fabrication and Measurement

This chapter introduces the complete design procedure of a compact two-stage bandpass filter with the specifications listed in Table 3.1 in greater detail based on the size reduction approach expatiated in last chapter to validate its availability. It should be noted that the number of stage mentioned in this thesis is not counted by the resonators as usual, but rather it is the inverter number of the generalized bandpass filter. In other words, an n-stage miniaturized bandpass filter means it consists of n pairs of coupled-line, and the inverter number is n. The first step is to obtain the circuit parameters of the one-stage bandpass filter according to the desired specifications and fine tune each element value. Then, two same tuned one-stage filters were cascaded through a connecting transmission line. After converting the circuit parameters to physical filter structures, some necessary tuning and optimizations were carried out to accommodate the parasitic effects of each lumped element, mutual coupling effects between elements, and finalize the layout design by employing full-wave electromagnetic (EM) simulation tool. Finally, the designed bandpass filter was fabricated with multilayer LTCC technology and carefully examined. In order to design the bandpass filter in a time-efficient way, we adopted both the circuit simulation software Agilent Advanced Design System (ADS) and full-wave 3-D EM simulation tool Ansoft HFSS to expedite the otherwise difficult work.

Table 3.1 Specifications of the proposed two-stage bandpass filter

Center frequency (GHz)	2.3 GHz
Fractional bandwidth (%)	10%
Insertion loss (dB)	-1.5 dB maximum
Stopband rejection (dB)	< -60 dB up to 3 f_0

3.1 Circuit simulation

3.1.1 One-stage bandpass filter design

A one-stage bandpass filter working at 2.3 GHz with 10% fractional bandwidth was designed in this subsection. Firstly, the initial miniaturized filter model illustrated in Fig. 2.6 with the electrical length of coupled-line being 10º was obtained. When the even-mode impedance Z_{0e} was arbitrarily chosen as 60 Ω, the value of the lumped capacitor C_L was calculated to be 7.9 pF according to the equations (2.6) and (2.9) and the odd-mode impedance of the coupled-line Z_{0o} was 42 Ω, making the coupling coefficient K being 0.18. The coupling coefficient $K = \frac{Z_{0e} - Z_{0o}}{Z_{0e} + Z_{0o}}$ of the short-ended coupled-line can determine the bandwidth of the proposed bandpass filter. The bandwidth increases as the coupling coefficient K does [23]. When the quarter-wavelength transmission line was miniaturized, one can choose a proper coupling coefficient according to the required bandwidth of the bandpass filter. However, to achieve a broad bandwidth, the coupling coefficient K should be made as large as possible, which means the difference between Z_{0e} and Z_{0o} should be large. It will result in a small Z' and hence a large electrical length of the coupled-line. Therefore, a necessary design

trade-off between broad bandwidth and small circuit size should be considered.

With the obtained circuit parameters, the ADS model of the initial size-reduced bandpass filter was built as given in Fig. 3.1 (a) and its frequency response is also shown in Fig. 3.1 (b), from which we can observe the great agreement with our expectation. It is worthy to be noted that there is no any spurious response appeared in the upper stopband.

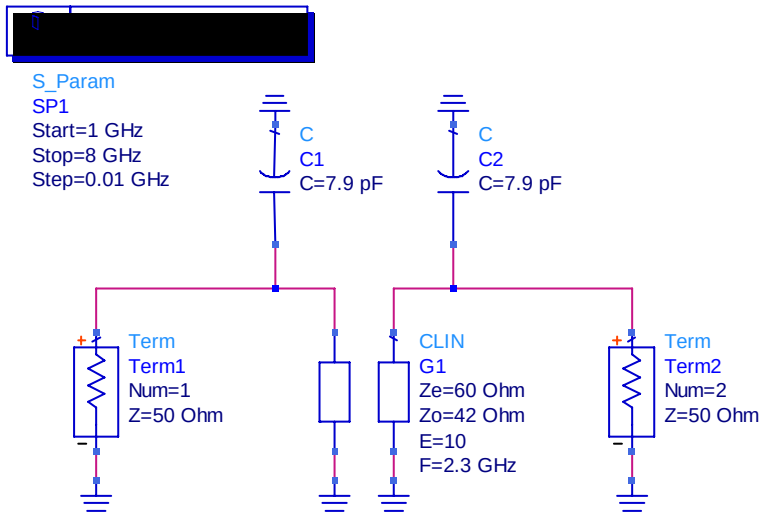

(a)

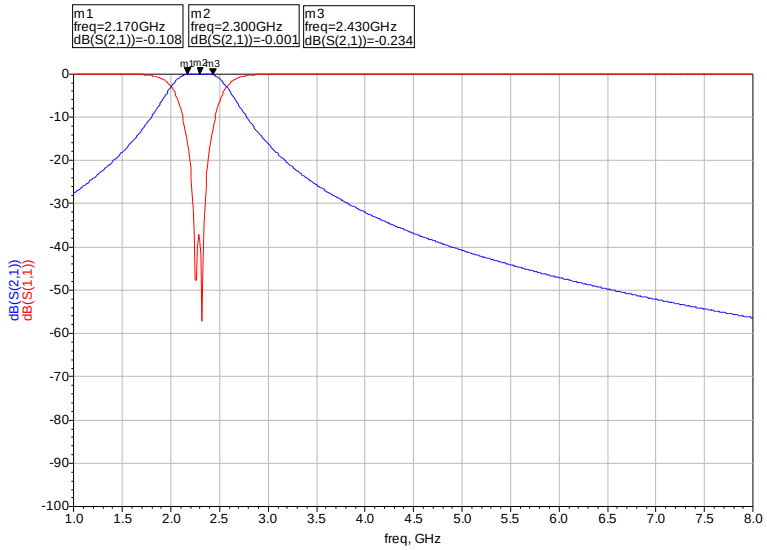

(b)

Fig. 3.1 The ADS model of the initial miniaturized one-stage bandpass filter (a) and its frequency response (b).

Then the cross-coupling capacitor C_C was inserted to realize a transmission zero at 4.6 GHz for better upper skirt characteristic and 2nd harmonic suppression. Depending on the desired location of the transmission zero, the value of this capacitor can be selected to meet the requirement. Fig. 3.2 shows the simulated filter responses for different values of the capacitor C_C. With nearly the same passband performance, the attenuation poles are located at the frequency of 3.3 GHz, 3.9 GHz, 4.6 GHz and 5.5 GHz when the capacitor values are 1.5 pF, 0.8 pF, 0.5 pF and 0.3 pF, respectively. However, one point that should be paid attention is the stopband attenuation levels differ in these cases. Using (2.11), the capacitance of C_C was calculated to be 0.44 pF; however, the utilization

of 0.5 pF capacitor was more proper according to the ADS simulation.

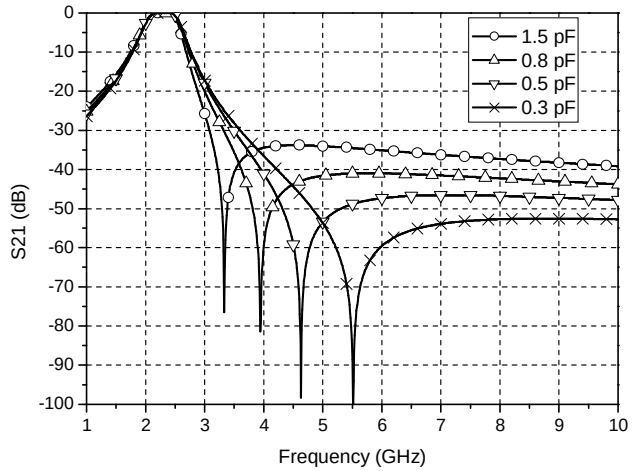

Fig. 3.2 The simulated frequency responses for different cross-coupling capacitors in ADS.

As mentioned above, the insertion of C_C leads to tight coupling and thus we have to decrease the odd-mode impedance Z_{0o} of the coupled-line, while the even-mode impedance Z_{0e} is kept the same. The resulted circuit can be optimized with ADS to achieve the desired filter responses. This optimization process is very time-efficient since it is a lumped element circuit simulation. A modified compact bandpass filter circuit was then obtained after the optimization, as shown in Fig. 3.3 (a), and Fig. 3.3 (b) is the corresponding frequency response. Here, the odd-mode impedance Z_{0o} of 36.6 Ω is the optimum value in this design.

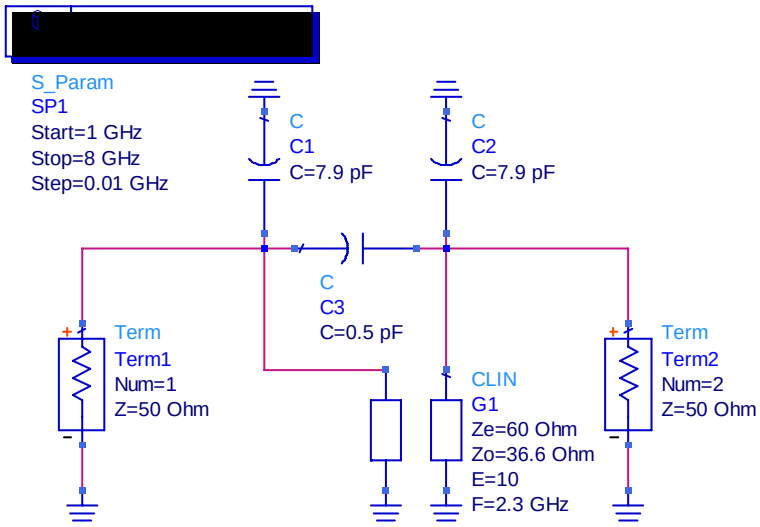

(a)

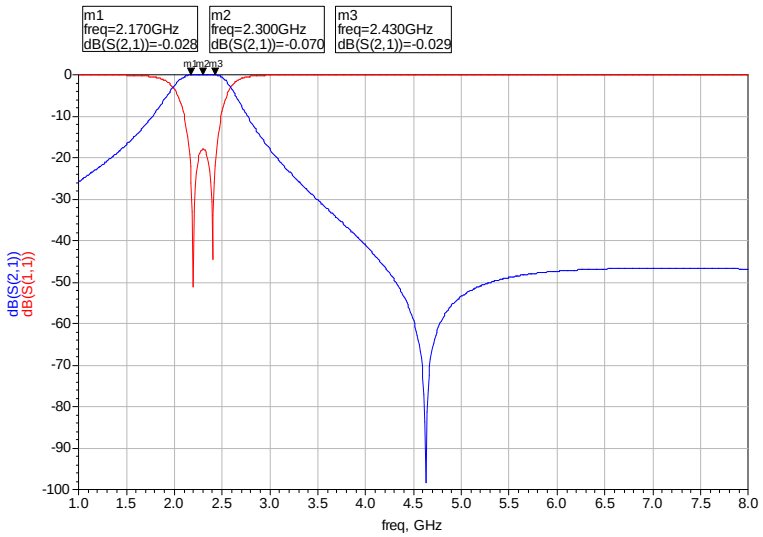

(b)

Fig. 3.3 The ADS model of the proposed compact one-stage bandpass filter with a transmission zero (a) and its frequency response (b).

The comparison of ADS simulated results of the initial miniaturized one-stage bandpass filter and its modified version is also given in Fig. 3.4. Obviously, without affecting the fundamental frequency response, the latter filter performance was improved significantly as we expected by trading off the attenuation level at the far end of the upper stopband and there is no any spurious response appeared.

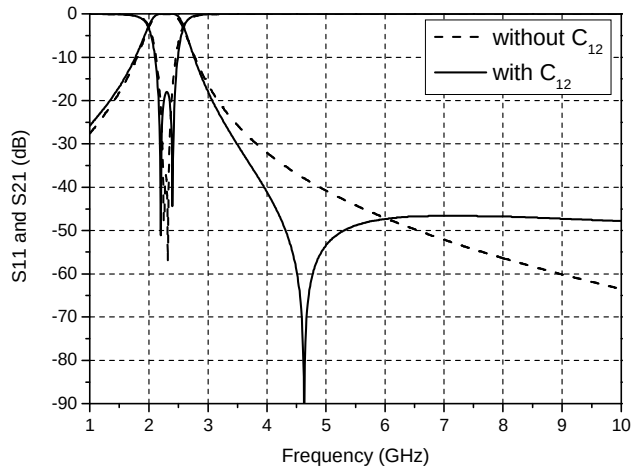

Fig. 3.4 The simulated frequency responses of both the initial miniaturized bandpass filter and its modified version in ADS.

3.1.2 Cascading for two-stage bandpass filter

The final two-stage bandpass filter can be achieved by simply connecting two same obtained circuits in last subsection using a short transmission line. However, this connecting line will generate an extra spurious response unless its electrical length is 0°, which is impossible in the practical situation. Fig. 3.5 (a) and (b) illustrate the spurious response

in both cases of cascading the initial miniaturized one-stage bandpass filter and cascading its modified version with a transmission zero.

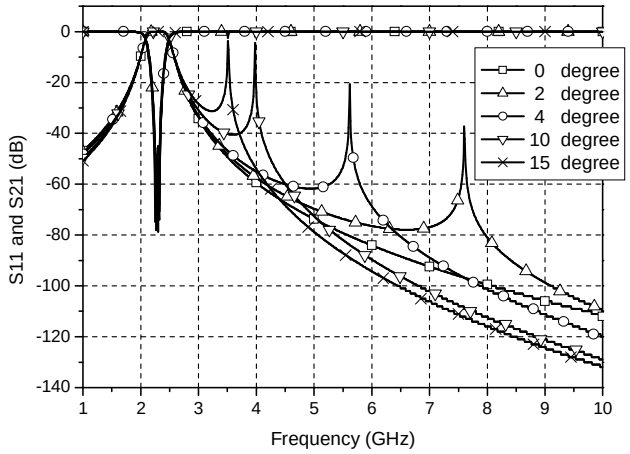

(a)

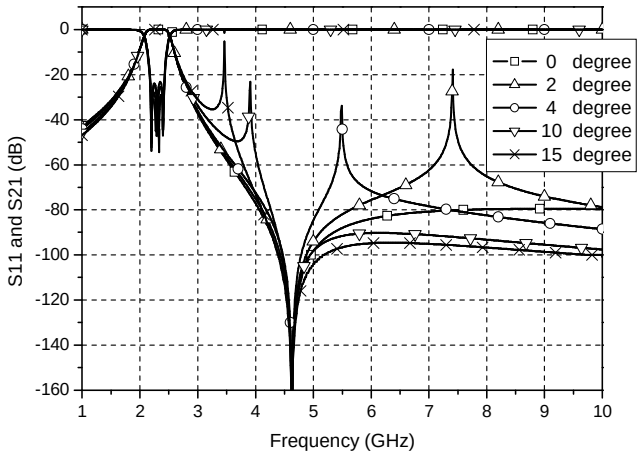

(b)

Fig. 3.5 The spurious response resulted from the connecting transmission line: cascading the initial miniaturized one-stage bandpass filter (a) and cascading its modified version with a transmission zero (b).

The particular studies on the connecting transmission line have been done with ADS. It is found that the location of this spurious band is closely related to the electrical length and the impedance of the connecting line, thus we can shift the peak of spurious band to the transmission zero frequency to suppress it.

Fig. 3.6 (a), which gives the simulated results according to different electrical length of the connecting line with same impedance of 50 Ω, indicates that the longer electrical length causes the shift of the spurious band peak to a lower frequency. Fig. 3.6 (b) is the frequency responses responding to different impedance of the connecting line with same electrical length of 6.15°. It can be seen that the higher impedance of the connecting transmission line, the peak of the spurious band moves to a lower frequency. Therefore, according to the simulation, a connecting transmission line with the electrical length of 6.15° and the impedance of 50 Ω, which can move the peak of spurious band to the 2nd harmonic frequency, is adopted for making the undesired response disappear in this design. The final two-stage bandpass filter circuit and its ADS simulated results are shown in Fig. 3.7 (a) and (b).

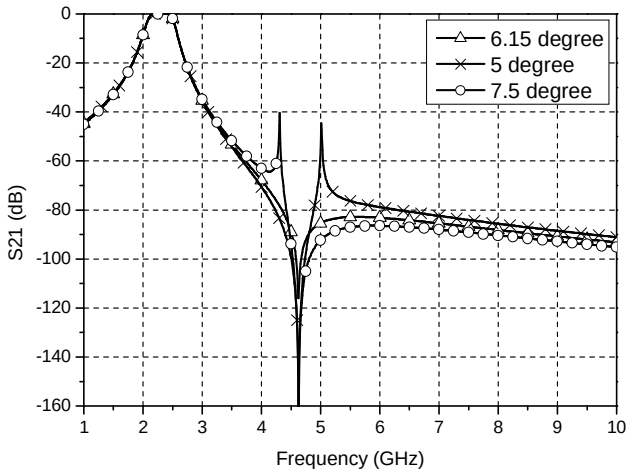

(a)

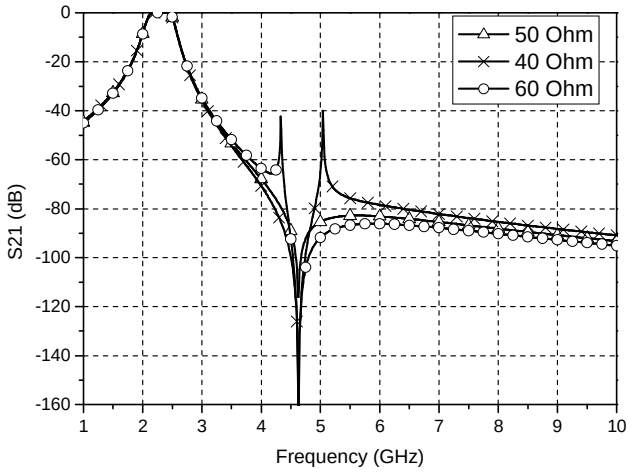

(b)

Fig. 3.6 The simulated frequency responses according to the electrical length of the connecting line (a) and the impedance of the connecting line (b) in ADS.

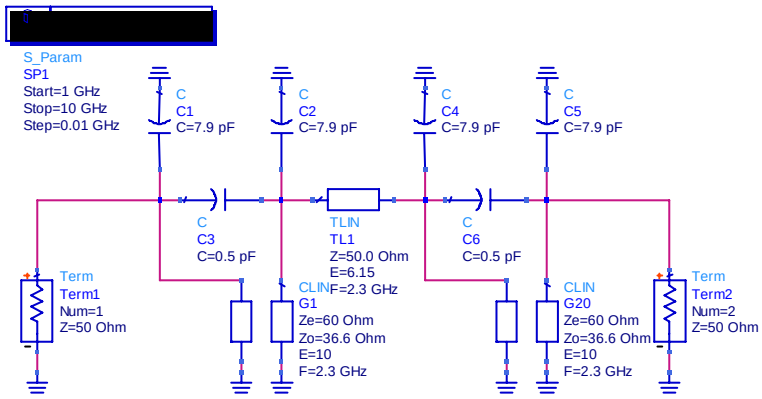

(a)

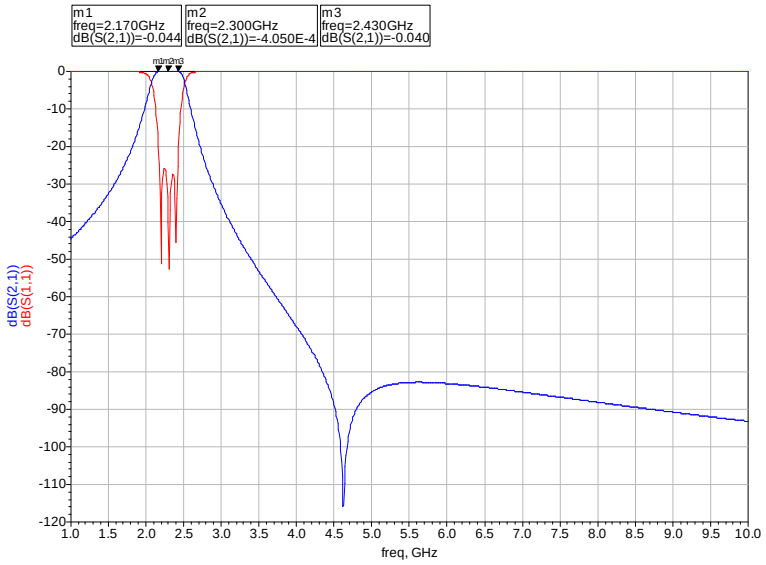

(b)

Fig. 3.7 The ADS model of the final compact two-stage bandpass filter (a) and its frequency response (b).

3.2 Full-wave EM simulation and optimization

Once the bandpass filter equivalent circuit model was developed, physical filter structures such as resonators and coupled-line sections can be designed. However, one thing needs to be kept in mind: the synthesized filter model can not be transformed into physical structures at one shot due to the parasitic components (both internally and externally). As a result, either an optimization of the filter physical dimensions or a tuning of the filter responses is necessary. Usually, it is carried out with Ansoft HFSS until the EM simulation shows a performance close to the target one.

3.2.1 LTCC layout of the one-stage bandpass filter

Like the simulation procedure in ADS, firstly, a one-stage bandpass filter was implemented in a seven-layer LTCC substrate, which has a dielectric constant of 5.6 and a metal thickness of 15 μm. The distances between each metal layer are 585, 650, 20, 20, 650, and 200 μm consecutively from the top. Fig. 3.8 (a) displays the 3-D physical architecture. The parallel coupled-line is realized on layer 4 using stripline form because dispersion and radiation of a stripline are negligible and upper and lower ground planes provide effective shielding. The capacitors are implemented on layer 3, 4, and 5 using the simple metal–insulator–metal (MIM) structure. The detailed capacitor configuration schematic is available in Fig. 3.8 (b). Layer 2 and 6 are the stripline ground with rectangular configuration apertures over and underneath the coupled striplines. The minimum slot between the coupled stripline conductors is generally 100 μm with screen-printing LTCC process, which limits to make wanted tighter coupling. So this design

resorted to the aperture compensation technique to overcome it. The top and bottom ground shield the filter to minimize the interaction with other components, while the surrounding ground located on layer 4 takes the same effect. All of the ground layers are connected with the aid of two rows of periodic metallized via-holes with diameter of 200 μm. Since the input and output ports are located on the bottom layer, they are also connected to the resonators by via-holes. Silver are used for both strip conductor and via-holes conductor. It is worth noting that the metal area in the internal layer should be less than 50% according to the LTCC process design rule. Therefore, we have to increase the width of the overall filter, which results in a big size. On the other hand, however, this structure has an advantage of strong power-handling capability because of its ease of heat dissipation. The overall size of this one-stage bandpass filter is 6 × 7 × 2.2 mm^3, where the intrinsic area occupied by the resonator is only a half.

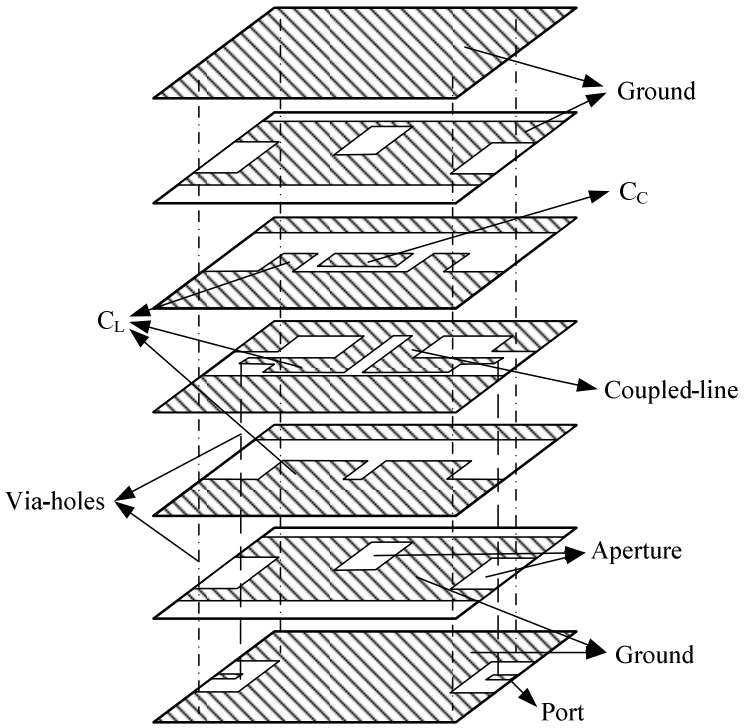

(a)

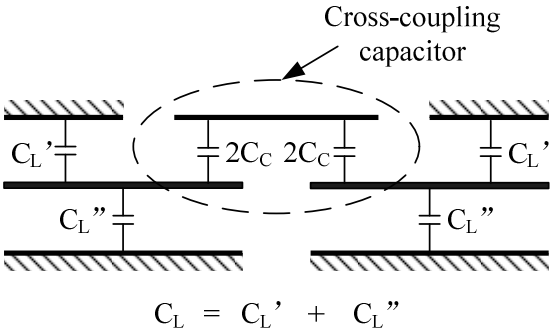

(b)

Fig. 3.8 LTCC layout of the designed one-stage bandpass filter (a) and the detailed capacitor configuration (b).

3.2.2 Influence of the PCB size

Considering the practical environment, the LTCC bandpass filter is mounted on the pad of a PCB, as illustrated in Fig. 3.9, with the signal feed composed of coplanar waveguide (CPW) feed line printed on the top of the PCB. Thus, the overall performance should include the parasitic of the PCB. To investigate the influence of the PCB size, full-wave 3-D EM simulator HFSS was conducted. Fig. 3.10 gives the simulated results of the one-stage bandpass filter without the PCB and with different PCB feed line length of 500, 5000 and 10000 μm, respectively. It is found from the simulation that the PCB size will affect the harmonic suppression performance and the matching condition of the designed filter. Moreover, the big size PCB will cause high insertion loss undoubtedly.

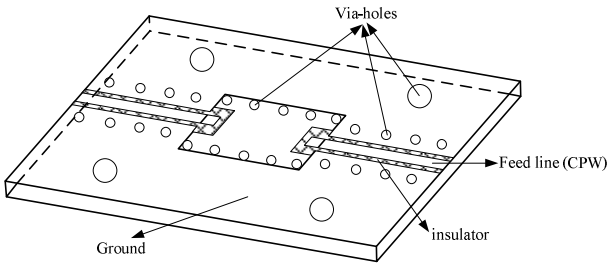

Fig. 3.9 The 3-D view of the PCB environment.

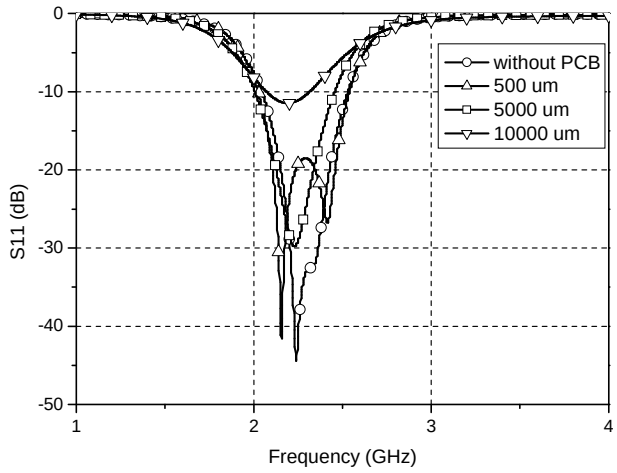

(a)

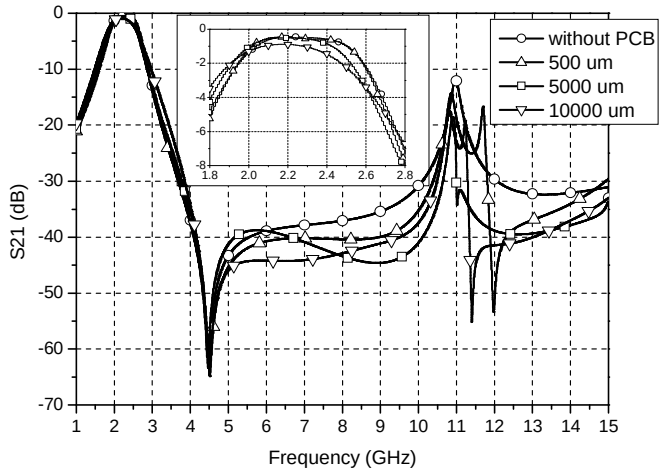

(b)

Fig. 3.10 The simulated results of the one-stage bandpass filter with different PCB feed line length: return loss (a) and insertion loss (b).

The one-stage bandpass filter responses including a small PCB with feed line of 500 μm after optimization in HFSS are given in Fig. 3.11. To show the details in passband, a zoom out view is also presented. An excellent agreement between the ADS simulation and the HFSS simulation can be observed, including a very low insertion loss of -0.55 $\pm$ 0.1 dB, good rejection at 2 f_0 due to the transmission zero and wide stopband rejection about -40 dB up to 10 GHz. It is believed that the stopband rejection level can be enhanced by cascading more stages.

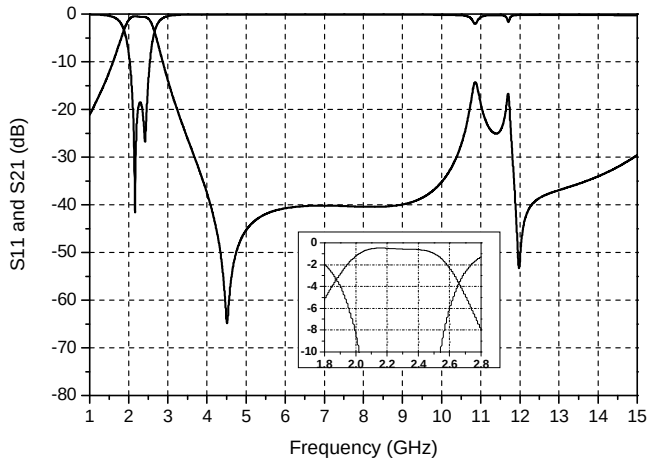

Fig. 3.11 The HFSS simulated results of the designed one-stage bandpass filter with a small PCB.

3.2.3 Two-stage bandpass filter simulation

After the geometrical parameters of the coupled-line, capacitors and ground plane apertures are obtained by fine tuning in HFSS, cascading was carried out for the final step. As can be seen from the top view of layer 4 in Fig. 3.12, two same one-stage bandpass filters were connected

reversely through a short transmission line for making the ports in the center.

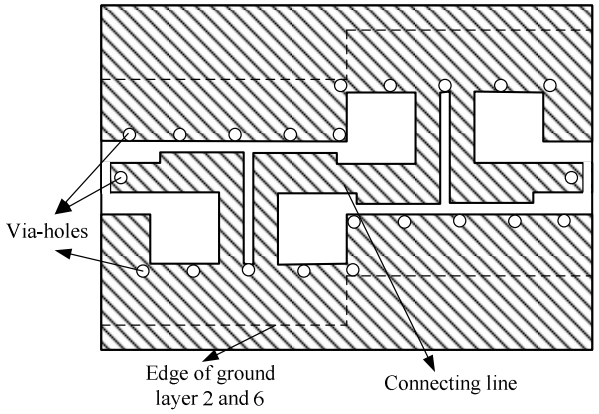

Fig. 3.12 The top view of the cascaded two-stage bandpass filter.

The filter responses simulated by HFSS are shown in Fig. 3.13, and the detailed passband responses are also plotted in the zoomed windows. This simulation was also carried out including a small PCB with feed line length of 500 μm. As can be seen, the designed filter exhibits a low insertion loss of -1.0 dB and good frequency selectivity. The return loss within the passband is less than -15 dB. Moreover, the rejection level is kept below -40 dB up to 12 GHz, which is 5 times of the center frequency (2.3 GHz) of the dominant passband, thus making up the attractive ultra-broad rejection of spurious passbands. Especially, due to the transmission zero created by cross-coupling capacitor, the 2nd harmonic attenuation is nearly -80 dB. We can observe that the filter responses simulated by the full-wave simulator are almost the same as the responses optimized by the circuit simulator ADS. This proves the validity of this

design method.

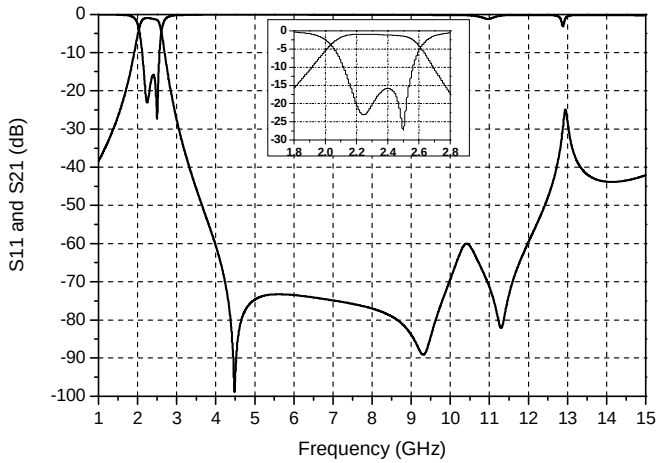

Fig. 3.13 The HFSS simulated results of the designed two-stage bandpass filter with a small PCB.

3.3 Fabrication and measurement

Having obtained the optimized structural parameters in the above section, the chip-type LTCC bandpass filter has been fabricated by RN2 Technologies. The dielectric constant of the LTCC raw material is 5.6 ± 0.2 and the used conductor is silver with thickness of 15 μm after firing and conductivity of 5.5×10^7 siemens/m. The via-hole is 200 μm in diameter. Fig. 3.14 shows the photograph of the fabricated bandpass filter mounted on PCB. The overall size is only $10 \times 7 \times 2.2$ mm^3. Fig. 3.15 (a) and (b) are the measured results in the wide frequency range of 50 MHz to 8 GHz and the narrow frequency range of 1.8 GHz to 2.8 GHz, respectively. The comparison between measured responses of the filter

and those from EM simulation is also presented in Fig. 3.15 (c).

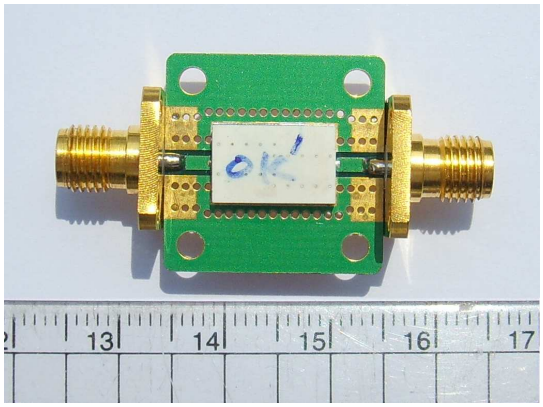

Fig. 3.14 The photograph of the fabricated two-stage bandpass filter mounted on PCB.

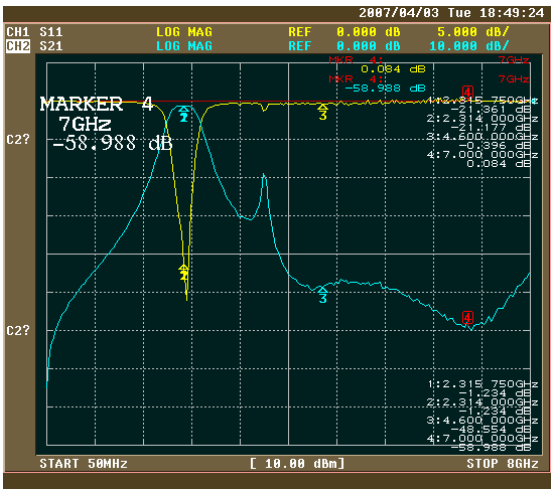

(a)

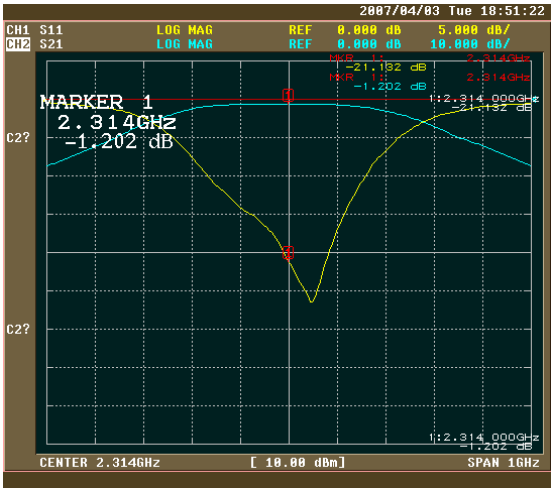

(b)

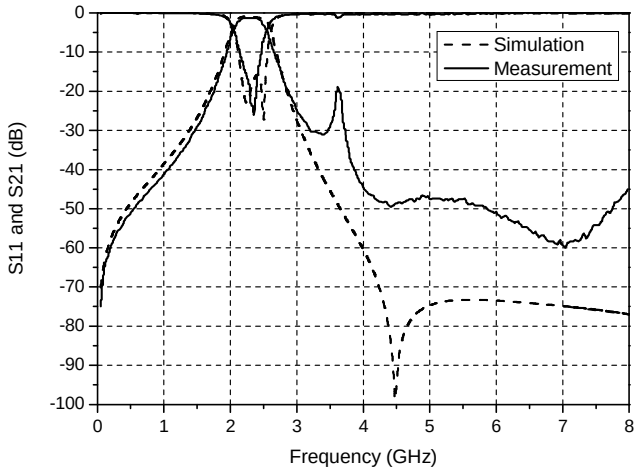

(c)

Fig. 3.15 The measured broad band performance of the fabricated two-stage bandpass filter mounted on PCB (a), the corresponding narrow band results (b) and the comparison of the measurement and simulation (c).

It can be seen that the measured center frequency and bandwidth matched well with the simulation. And in the passband, the insertion loss is found to be -1.2 dB, and the return loss is better than -15 dB. However, a small unwanted peak at the frequency point of 3.6 GHz appears resulted from the connecting transmission line. The rejection level at this point is -20 dB. This discrepancy probably comes from lack of accuracy in the fabrication process. Actually the printing process is capable of resolving a 150 μm line with 10% accuracy in LTCC technology. As to the out of band rejection, although it is not as excellent as the simulation due to the absence of transmission zero, the average attenuation of -50 dB up to 8 GHz is sufficient, which is nearly 4 times of the center frequency (2.3 GHz) of the dominant passband. Although the measured results are somewhat different from the simulated ones in the higher band, it still verifies the possibility of the proposed design concept.

Finally, Table 3.2 summarizes the characteristic of several published harmonic-suppression bandpass filters in comparison with this work. Obviously, the proposed bandpass filter in this thesis shows the advantage of more compact size, excellent insertion loss characteristic, and better stopband rejection performance.

Table 3.2 Comparison of the different types of harmonic-suppression bandpass filter

Refe-rence	Bandwidth and Center Frequency (GHz)	S_{11} (dB)	S_{21} (dB)	Harmonic Suppression Level	Overall Physical Size (mm× mm)	Electrical Length (deg)	Struc-ture	Technology	Year
[24]	3.8~9.9 (6.85)	<-12	-0.5	up to 20 GHz, better than -30 dB	19.5 × 11.5	-	2-D	Stepped-impedance resonator	2007
[25]	11.4~12.6 (12)	<-10	-2.8	up to 36 GHz, better than -30 dB	18.5 × 9.5	90	2-D	Half-wave open-ended and filter bent	2006
[26]	1.85~2.15 (2)	<-12	-2.8	up to 14 GHz, better than -30 dB	70.0 × 20.0	30	2-D	Open-ended and short-ended coupled-line sections	2008
[27]	1.4~1.5 (1.45)	<-14	-2.0	up to 4 GHz, better than -35 dB	25.0 × 25.0	-	2-D	Perturbed square-ring resonator	2006
[28]	0.96~1.04 (1)	<-15	-2.6	up to 18 GHz, better than -30 dB	140.0 × 10.0	45	2-D	Corrugated coupled-line and tapped input/output	2007

[16]	2.9~3.1 (3)	<-25	-1.5	up to 6 GHz, better than -40 dB	20.0 × 15.0	90	2-D	Coupled-line with DGS	2002
[29]	1.85~2.15 (2)	-	-2.6	up to 10 GHz, better than -30 dB	120.0 × 30.0	90	2-D	Coupled-line with rectangular PBG loops	2005
[30]	3.4~5.0 (4.2)	<-20	-0.6	up to 12 GHz, better than -25 dB	10.0 × 5.0	-	2-D	Open-ended stub and DGS	2004
[31]	3.8~4.1 (3.95)	<-20	-1.5	up to 16 GHz, better than -40 dB	20.0 × 3.0	90	2-D	Aperture-backed Stepped-impedance resonator	2005
This work	2.18~2.42 (2.3)	<-15	-1.2	up to 8 GHz, better than -40 dB	10 × 7 × 2.2	10	LTCC	Short-ended coupled-line with capacitive loading and cross-coupling	2008

CHAPTER 4 Conclusion

A novel implementation and associated design formulas for a compact multi-harmonic suppression bandpass filter are proposed in this thesis. The proposed filter is based on the structure of capacitive loading of the parallel short-ended coupled-line, which is a relatively simple mean of reducing the coupled-line electrical length that usually plays a decisive role to the filter size. On the other hand, the use of lumped elements can effectively suppress the spurious passbands. By introducing the cross-coupling capacitor into the miniaturized coupled-line section, a transmission zero can be generated to achieve better frequency selectivity and wide multi-harmonic suppression. The location of the transmission zero may easily be adjusted by varying the cross-coupling capacitance. In addition, the aperture compensation technique is also applied for tight coupling in the coupled-line section. Although this filter schematic is well known, a different design approach is presented. The approach cascades two identical elementary filters to achieve the desired specifications, making the design procedure simple and providing design flexibility. Moreover, this method is general and geometry-independent, thus can be applied to any type of bandpass filter design.

The proposed bandpass filter has been successfully realized using LTCC technology in a seven-layer ceramic substrate. This filter exhibits not only an excellent spurious passband rejection of better than -40 dB in

the upper stopband even up to 4 f_0, but also low insertion loss of -1.2 dB and good frequency selectivity, showing promising application potentials. To certify this approach, such a two-stage bandpass filter with low insertion loss and sufficient multi-harmonic suppression was fabricated and carefully examined. Measurement and predicted results in the 3-D simulation are found in good agreement with each other, showing that the proposed design method is very effective in high-performance bandpass filter design.

References

[1] S. B. Cohn, "Parallel-coupled transmission-line resonator filters," *IRE Trans.*, vol. MTT-6, no. 4, pp. 223-231, Apr. 1958.

[2] J. S. Hong and M. J. Lancaster, "Cross-coupled microstrip hairpin resonator filters," *IEEE Trans. Microw. Theory Tech.*, vol. 46, no. 1, pp. 118-122, Jan. 1998.

[3] M. Sagawa, K. Takahashi and M. Makimoto, "Miniaturized hairpin resonator filters and their application to receiver front-end MIC's," *IEEE Trans. Microw. Theory Tech.*, vol. 37, no. 12, pp. 1991-1997, Dec. 1989.

[4] A. Djaiz and T. A. Denidni, "A new compact microstrip two-layer bandpass filter using apertured-coupled SIR-hairpin resonators with transmission zeros," *IEEE Trans. Microw. Theory Tech.*, vol. 54, no. 5, pp. 1929-1936, May. 2006.

[5] M. Makimoto and S. Yamashita, "Bandpass filters using parallel coupled strip-line stepped impedance resonators," *IEEE Trans. Microw. Theory Tech.*, vol. 28, no. 12, pp. 1413–1417, Dec. 1980.

[6] J. T. Kuo and E. Shih, "Microstrip stepped impedance resonator bandpass filter with an extended optimal rejection bandwidth," *IEEE Trans. Microw. Theory Tech.*, vol. 51, no. 5, pp. 1554-1559, May. 2003.

[7] X. Wang, P. Liu and Y. Li, "New compact configuration of a stepped-impedance ceramic bandpass filter," *Microw. Opt. Technol. Lett.*, vol. 41, no. 2, pp. 146-149, Apr. 2004.

[8] J. S. Hong and M. J. Lancaster, "Theory and experiment of novel microstrip slow-wave open-loop resonator filters," *IEEE Trans. Microw. Theory Tech.*, vol. 45, no. 12, pp. 2358–2365, Dec. 1997.

[9] J. S. Hong and M. J. Lancaster, “Cross-coupled microstrip square open-loop resonators for cross-coupled planar microwave filters,” *IEEE Trans. Microw. Theory Tech.*, vol. 44, no. 11, pp. 2099–2109, Nov. 1996.

[10] E. Pistono, M. Robert and L. Duvillaret, “Compact fixed and tune-all bandpass filters based on coupled slow-wave resonators,” *IEEE Trans. Microw. Theory Tech.*, vol. 54, no. 6, pp. 2790-2799, Jun. 2006.

[11] J. T. Kuo, S. P. Chen and M. Jiang, “Parallel-coupled microstrip filters with over-coupled end stages for suppression of spurious responses,” *IEEE Microw. Wireless Compon. Lett.*, vol. 13, no. 10, pp. 440-442, Oct. 2003.

[12] T. Lopetegi and M. A. G. Laso, “New microstrip wiggly line filters with spurious passband suppression,” *IEEE Trans. Microw. Theory Tech.*, vol. 49, no. 9, pp. 1593-1598, Sep. 2001.

[13] S. M. Wang, C. H. Chi and M. Y. Hsieh, “Miniaturized spurious passband suppression microstrip filter using meandered parallel coupled lines,” *IEEE Trans. Microw. Theory Tech.*, vol. 53, no. 2, pp. 747-753, Feb. 2005.

[14] J. T. Kuo, M. Jiang and H. J. Chang “Design of parallel-coupled microstrip filters with suppression of spurious resonances using substrate suspension,” *IEEE Trans. Microw. Theory Tech.*, vol. 52, no. 1, pp.83-89, Jan. 2004.

[15] J. Yoon and C. Seo, “Improvement of broadband feedforward amplifier using photonic bandgap,” *IEEE Microw. Wireless Compon. Lett.*, vol. 11, no. 11, pp. 450–452, Nov. 2001.

[16] J. S. Park, J. S. Yun and D. Ahn, “A design of the novel coupled line bandpass filter using defected ground structure with wide stopband performance,” *IEEE Trans. Microw. Theory Tech.*, vol. 50, no. 9, pp. 2037–2043, Sep. 2002.

[17] C. W. Tang, Y. C. Lin and C. Y. Chang, “Realization of transmission zeros in combline filters using an auxiliary inductively coupled ground plane,” *IEEE Trans. Microw. Theory Tech.*, vol. 51, no. 10, pp. 2112-2118, Oct. 2003.

[18] C. W. Tang and S. F. You, "Design Methodologies of LTCC bandpass filters, diplexer, and triplexer with transmission zeros," *IEEE Trans. Microw. Theory Tech.*, vol. 54, no. 2, pp. 717-723, Feb. 2006.

[19] L. K. Yeung and K. L. Wu, "A compact second-order LTCC bandpass filter with two finite transmission zeros," *IEEE Trans. Microw. Theory Tech.*, vol. 51, no. 2, pp. 337–341, Feb. 2003.

[20] G. L. Matthaei, L. Young and E. M. T. Jones, *Microwave Filters, Impedance Matching Networks and Coupling Structures*, Artech House Inc., Norwood MA, 1980.

[21] I. H. Kang and J. S. Park, "A reduced-size power divider using the coupled line equivalent to a lumped inductor," *Microwave Journal*, vol. 46, no. 7, Jul. 2003.

[22] D. M. Pozar, *Microwave Engineering*, Addison-Wesley Publishing Company, Inc., pp. 415-419, 1990.

[23] I. H. Kang and K. Wang, "A broadband rat-race ring coupler with tightly coupled lines," *IEICE Trans. Commun.*, vol. E88-B, no. 10, pp. 4087-4089, Oct. 2005.

[24] H. N. Shaman and J. S. Hong, "Compact wideband bandpass filter with high performance and harmonic suppression," in *Proc. of the 37th European Microwave Conference*, Munich Germany, pp. 528–531, Oct. 2007.

[25] S. Hong and K. Chang, "A parallel-coupled microstrip bandpass filter with suppression of both the 2nd and the 3rd harmonic responses," in *IEEE MTT-S Int. Microw. Symp. Dig.*, pp. 365–368, Jun. 2006.

[26] Y. S. Lin, P. Y. Chang and Y. S. Hsieh, "Compact electronically switchable parallel-coupled microstrip bandpass filter with wide stopband," *IEEE Microw. Wireless Compon. Lett.*, vol. 18, no. 4, pp. 254–256, Apr. 2008.

[27] X. D. Huang and C. H. Cheng, "A novel microstrip dual-mode bandpass filter with harmonic suppression," *IEEE Microw. Wireless Compon. Lett.*, vol. 16, no. 7, pp. 404–406, Jul. 2006.

[28] J. T. Kuo, U. H. Lok and M. H. Wu, "Novel corrugated coupled-line stage with ideal frequency response and its application to bandpass filter design

with multi-harmonic suppression," in *IEEE MTT-S Int. Microw. Symp. Dig.*, pp. 553–556, 2007.

[29] M. H. Weng, R. Y. Yuan, T. H. Huang, H. J. Chen, W. N. Chen and M. P. Houng, "Spurious suppression of a microstrip bandpass filter using three types of rectangular PBG loops," *IEEE Trans. Ultrasonics, Ferroelectrics, and Frequency Control*, vol. 52, no. 3, pp. 487–490, Mar. 2005.

[30] A. Abdel-Rahman, A. K. Verma, A. Boutejdar and A. S. Omar, "Compact stub type microstrip bandpass filter using defected ground plane," *IEEE Microw. Wireless Compon. Lett.*, vol. 14, no. 4, pp. 136–138, Apr. 2004.

[31] H. Wang and L. Zhu, "Microstrip bandpass filter with ultra-broad rejection band using stepped impedance resonator and high-impedance transformer," in *IEEE MTT-S Int. Microw. Symp. Dig.*, pp. 683–686, Jun. 2005.

Acknowledgement

I would like to acknowledge a number of people who have helped me during the past two years. There is no way for me to finish this thesis without their supports and encouragements.

First and foremost, my greatest appreciation surely belongs to Prof. In-Ho Kang, who guided me through the M.S. program. His creativity, broad knowledge and insight into the circuit design helped me avoid going down wrong path and shortened the path to achieve the project goal. His energy and love of what he is doing inspires me a lot. I feel very grateful for his supervision both on the technical and the personal levels during my stay at Busan.

I would also like to express my sincere gratitude to the other professors of our department for their guidance, who are Prof. Dong-Il Kim, Prof. Hyung-Rae Cho, Prof. Ki-Man Kim, Prof. Young Yun, Prof. Kyeong-Sik Min and Prof. Ji-Won Jung. I am particularly grateful to my thesis committee members Prof. Ki-Man Kim and Prof. Young Yun for their time and valuable suggestions in guiding and reviewing my work. My acknowledgement will not be complete without mentioning the staff members of the Department of Radio Science and Engineering for their dedication and assistance.

I want to thank all the past and present members of the RF Circuit & System Lab, especially Mr. Kai Wang and Mr. Hong-Chao Zhang, for their professional and personal supports. A special note of thanks goes to Mr. Rui Li, my senior in the same department, for lots of help and productive discussions with RF circuit design. There is also my gratitude to all other friends at Korea Maritime University for the friendly environment and emotional supports. I will not forget the time we spent together before and in the future.

Additionally, I am deeply indebted to Prof. Ying-Ji Piao at Qingdao University. Without her recommendation, it is impossible for me to get this great opportunity to study in Korea.

Finally, I would like to dedicate this thesis to my family for their continued love and strong supports throughout all these years. You are always the persons who believe in and encourage me in all my endeavors, which is a contributing factor to any success I may achieve. Without these endless and priceless loves, it will never be possible for me to still live happily and accomplish my tasks. I feel great fortune to have you all accompany with me, only in this way, my life is complete and honorable.